

## Diffusion of Cations in Chromia Layers Grown on Iron-Base Alloys

R. E. Lobnig,\* H. P. Schmidt,\*\* K. Hennesen,\* and H. J. Grabke\*

Received May 31, 1991

---

*Diffusion of the cations Cr, Fe, Mn, and Ni in  $\text{Cr}_2\text{O}_3$  has been investigated at 1173 K. The diffusion measurements were performed on chromia layers grown on the model alloys Fe-20Cr and Fe-20Cr-12Ni in order to consider effects of small amounts of dissolved alien cations in  $\text{Cr}_2\text{O}_3$ . The samples were diffusion annealed in  $\text{H}_2$ - $\text{H}_2\text{O}$  at an oxygen partial pressure close to the  $\text{Cr}_2\text{O}_3$ /Cr equilibrium. For all tracers the lattice-diffusion coefficients are 3-5 orders of magnitude smaller than the grain-boundary diffusion coefficients. The lattice diffusivity of Mn is about two orders of magnitude greater than the other lattice-diffusion coefficients, especially in  $\text{Cr}_2\text{O}_3$  grown on Fe-20Cr-12Ni. The values of the diffusion coefficients for Cr, Fe, and Ni are in the same range. Diffusion of the tracers in  $\text{Cr}_2\text{O}_3$  grown on different alloys did not show significant differences with the exception of Mn.*

---

**KEY WORDS:** chromia layer; alien cation diffusion; lattice diffusion; grain-boundary diffusion; external spinel or sulfide growth.

### INTRODUCTION

In many technological processes at elevated temperatures, iron- and nickel-base alloys are used with chromium as a major constituent. Under oxidizing conditions, chromium is preferentially oxidized to form slow-growing, dense, and well-adherent chromia layers, leading to good corrosion resistance. A preoxidation treatment, under conditions where iron- and nickel-oxides and

\*Max-Planck-Institut für Eisenforschung GmbH, 4000 Düsseldorf, Germany.

\*\*Present affiliation: Messer Griesheim, Krefeld, Germany.

iron-chromium spinels are not stable but chromia can be formed, improves the protectiveness of the oxide scale even more.

To understand the effect of a chromia layer on the corrosion process, the transport properties of chromia must be known. Not only the diffusivities of chromium and oxygen in the  $\text{Cr}_2\text{O}_3$  layer are of interest but also the diffusion of alien cations and transport of nonmetal elements. The outward diffusion of cations such as Fe, Ni, and Mn from the alloy through the chromia layer plays a role in the growth of the outer spinel layer in the oxidation of high-alloy steels at high oxygen pressures (Fig. 1a); but also in sulfidizing atmospheres at low oxygen pressures, outward diffusion of these cations occurs leading to external sulfide growth (Fig. 1b). In coal-gasification atmospheres external sulfidation, i.e., growth of sulfides of the alloying elements Fe, Mn, Cr, and Ni on top of the scale, correlated to the outward diffusion of Fe, Mn, Ni, and Cr through the chromia scale, appears to be the major problem, leading to deterioration of the materials.<sup>1-5</sup>

The inward diffusion of nonmetallic elements such as carbon,<sup>6,7</sup> sulfur,<sup>8,9</sup> chlorine,<sup>10</sup> etc. generally is minor in a dense chromia layer, since their solubility in chromia is undetectably small<sup>6-10</sup> and transport is possible only through defects of the scale, pores, and cracks.

Several tracer studies have been performed previously on the diffusion of Cr and O in sintered or hot-pressed polycrystalline  $\text{Cr}_2\text{O}_3$ ,<sup>11-13</sup> as seen in Fig. 2. Lillerud and Kofstad<sup>14</sup> calculated chromium self-diffusion coefficients from evaporation experiments, i.e., from the mass loss during vacuum annealing of preoxidized chromium specimens. The diffusion coefficients resulting from these investigations include contributions of lattice- and grain-boundary diffusion and probably short-circuit diffusion in pores and cracks.

Walters and Grace,<sup>15</sup> Hoshino and Peterson,<sup>16</sup> Atkinson and Taylor,<sup>17</sup> and Schwanke<sup>18</sup> investigated the diffusion of Cr in chromia single crystals at different temperatures and oxygen pressures. In these studies, the influence

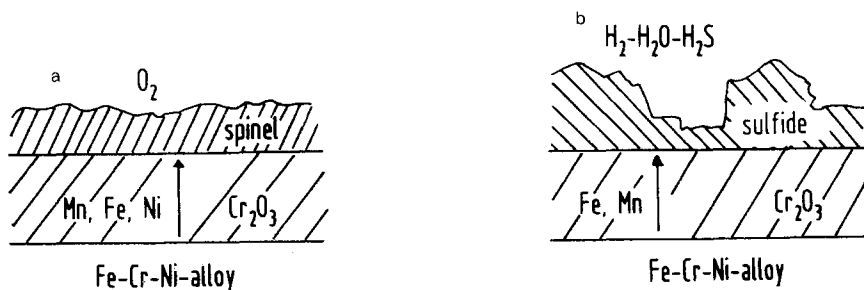


**Fig. 1.** (a) Schematic diffusion processes during oxidation of alloys with high chromium contents at high oxygen pressures. (b) Schematic diffusion processes during sulfidation/oxidation of preoxidized alloys with high chromium contents at low oxygen pressures.

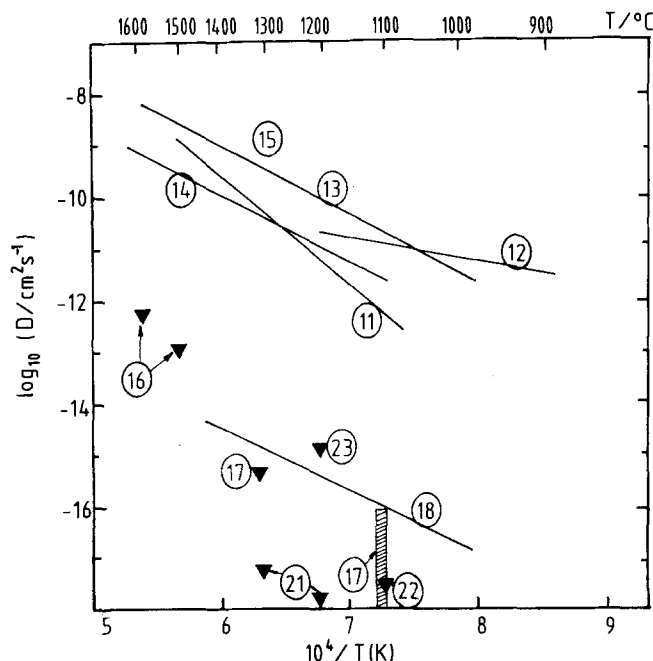


Fig. 2. Prior results of diffusion of chromium in chromia. The older values include volume- and grain-boundary diffusion; the more recent studies are volume-diffusion coefficients (see text and Table I). The numbers give the reference number.

of the faster grain-boundary diffusion is excluded, therefore the values of O- and Cr-diffusion coefficients are some orders of magnitude smaller than the data evaluated from studies with polycrystalline materials (see Fig. 2). The values are strongly dependent on oxygen pressure. The dependence indicates a change of the defect structure of  $\text{Cr}_2\text{O}_3$  with changing oxygen pressure.<sup>17-19</sup> The oxygen-diffusion coefficients determined more recently in air<sup>18,20</sup> are some orders of magnitude smaller than the values for chromium diffusion. These results are in agreement with the observation that chromia scales on high-temperature alloys grow by outward diffusion of chromium.<sup>17,19</sup> As lattice diffusion of chromium is at least three orders of magnitude too slow to explain the rate of chromia-scale growth, grain-boundary diffusion must be decisive for chromia-scale growth. Atkinson and Taylor<sup>17</sup> also took into consideration a contribution of diffusion along dislocations, i.e., low-angle boundaries in the oxide. According to their calculations, diffusion of Cr in low-angle boundaries is about three orders of magnitude faster than lattice diffusion. Sockel<sup>20</sup> determined lattice- and

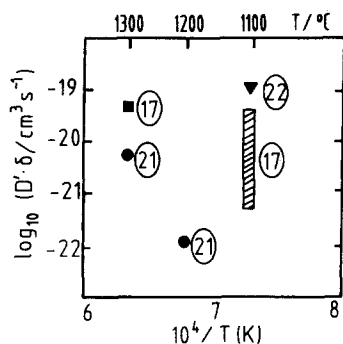


Fig. 3. Prior results on grain-boundary diffusion of chromium in chromia with  $D'$  grain-boundary diffusion coefficient and  $\delta$  grain-boundary width. The numbers indicate the reference number.

grain-boundary diffusion coefficients of  $^{18}\text{O}$  in polycrystalline chromia. The resulting grain-boundary diffusion coefficients are four orders of magnitude higher than those for lattice diffusion. Sabioni *et al.*<sup>21</sup> measured Cr grain-boundary diffusion in polycrystals of  $\text{Cr}_2\text{O}_3$ . They found a difference between lattice-diffusion coefficients obtained from measurements with single crystals and grain-boundary diffusion coefficients of 3–4 orders of magnitude.

Park *et al.*<sup>22</sup> investigated the diffusion of Cr in sintered polycrystals of  $\text{Cr}_2\text{O}_3$  and took contributions of lattice diffusion, of grain-boundary diffusion and of diffusion along the subboundary network into consideration. Figure 3 gives an overview on the determined values for  $D' \cdot \delta$  with  $D' =$  grain-boundary diffusion coefficient and  $\delta =$  grain boundary width.

Table I gives a summary of the conditions of previous diffusion studies. Up to now there are only a few direct investigations on the diffusion of Mn,

Table I. Conditions Applied in Previous Diffusion Studies of Cr in  $\text{Cr}_2\text{O}_3$

Author	Reference	Samples	Atmosphere
Lindner and Akerstrom (1956)	11	Sintered polycrystals	
Ignatov <i>et al.</i> (1958)	12	Sintered polycrystals	Vacuum
Hagel and Seybolt (1961)	13	Hotpressed polycrystals	Dried $\text{N}_2$
Walters and Grace (1965)	15	$\text{Cr}_2\text{O}_3$ -monocrystals	$\text{H}_2/\text{H}_2\text{O}$
Kinloch (1970)	23	$\text{Cr}_2\text{O}_3$ -monocrystals	$\text{CO}/\text{CO}_2$
Lillerud and Kofstad (1982)	14	Preoxidized chromium	Vacuum
Hoshino and Peterson (1983)	16	Preoxidized chromium	Vacuum
Atkinson and Taylor (1985)	17	Preoxidized chromium	Vacuum
Schwanke (1986)	18	Preoxidized chromium	$\text{H}_2/\text{H}_2\text{O}$ $\text{Ar}/\text{O}_2$
Sabioni <i>et al.</i>	21	Hotpressed polycrystals	Argon
Park <i>et al.</i> (1987)	22	Sintered polycrystals	Argon with $\text{Cr}/\text{Cr}_2\text{O}_3$

**Table II.** Diffusion Coefficients of  $^{55}\text{Fe}$  in  $\text{Cr}_2\text{O}_3$ -Monocrystals at 1473 K<sup>23</sup>

$P_{\text{O}_2}/\text{bar}$	$D/10^{-16} \text{ cm}^2 \text{ s}^{-1}$ crystallographic direction	
	<sup>a</sup> hex	<sup>c</sup> hex
0.21 (air)	50	220
$5 \times 10^{-6}$ (argon)	13	14
$6.3 \times 10^{-10}$ ( $\text{CO}_2$ -12.5% $\text{CO}$ )	11	40
$3.2 \times 10^{-13}$ ( $\text{CO}$ -12.5% $\text{CO}_2$ )	1.7	13

Fe, and Ni in  $\text{Cr}_2\text{O}_3$ . Ignatov<sup>12</sup> determined the diffusion coefficients of Fe in polycrystalline chromia in vacuum, he reported a diffusion coefficient of  $D_{\text{Fe}} = 4.95 \times 10^{-6} \exp(-44,000 \text{ cal/mol}/RT)$ . Kinloch<sup>23</sup> used  $^{55}\text{Fe}$  and  $\text{Cr}_2\text{O}_3$  monocrystals. According to this study, the  $D_{\text{Fe}}$  values are oxygen-pressure dependent, too. The values are given in Table II. The studies described show that for a quantitative description of transport processes in  $\text{Cr}_2\text{O}_3$ , especially at temperatures below 1273 K, grain-boundary diffusion must be taken into account. As it is very difficult to obtain polycrystalline chromia samples without pores by sintering or hot-pressing, diffusion coefficients from measurements with such materials will be affected by diffusion along fast diffusion paths like pores and therefore the values determined are too high. Therefore, the diffusion measurements in this study were performed on chromia layers grown on alloys. In this way also, the effects of small amounts of dissolved alien cations in as-grown oxide layers are considered. Chromia layers grown on iron- or nickel-base alloys can dissolve small amounts of iron or nickel, and therefore have a defect structure different from pure chromia.

The aim of this study was to estimate lattice- and grain-boundary diffusion coefficients of Cr, Fe, Ni, and Mn in  $\text{Cr}_2\text{O}_3$  scales grown on high-temperature alloys. Instead of outward diffusion as in practice (Fig. 1), here the inward diffusion was determined from layers evaporated onto grown  $\text{Cr}_2\text{O}_3$  layers; such experiments should lead to similar diffusivities.

## EXPERIMENTAL PROCEDURES

To obtain  $\text{Cr}_2\text{O}_3$  scales with similar properties like those grown on high-temperature alloys in technical atmospheres, model alloys Fe-20Cr and Fe-20Cr-12Ni were used. A Cr-content of 20% is suitable because, at higher Cr concentrations, the porosity of the chromia scale increases and at lower Cr concentrations, the  $\text{Cr}_2\text{O}_3$  scales are less adherent on the substrate, and Cr depletion below the scale is possible.<sup>6</sup> Samples of both alloys were cut to size ( $1 \times 2 \times 0.2 \text{ cm}$ ) from ingot materials and were abraded and polished from 400 mesh grit SiC through  $2.5 \mu\text{m}$  diamond.

The materials contain the following impurities (in wt. ppm at a level  $>40$  ppm): (1) Fe-20Cr: 86 ppm C-47 ppm S-330 ppm Si, and (2) Fe-20Cr-12Ni: 110 ppm C-88 ppm S. The samples were oxidized in  $\text{H}_2$ - $\text{H}_2\text{O}$  mixtures for 175 hr at 1173 K and  $P_{\text{O}_2} = 10^{-21}$  bar. Under these conditions,  $\text{Cr}_2\text{O}_3$  is the only stable oxide that can be formed on Fe-20Cr and Fe-20Cr-12Ni. The required oxygen pressure was established by a well-defined mixture of  $\text{H}_2$  and  $\text{H}_2\text{O}$ , which was passed through the furnace at a constant flow rate in order to avoid depletion of the gases.

The  $\text{Cr}_2\text{O}_3$  layers had a thickness of 1–2  $\mu\text{m}$ , as was deduced from the mass increase upon oxidation which was recorded by an electronic microbalance. The correctness of the values of scale thickness calculated from the mass change was proved by SEM investigations of cross-sections of oxidized samples. Figure 4 shows the surface of an oxidized Fe-20Cr sample (SEM).

A thin layer of the tracer was deposited on the surface of the chromia layer by evaporation in a UHV apparatus. For  $\text{Cr}_2\text{O}_3$  layers grown on Fe-20Cr the tracers  $^{54}\text{Fe}$ ,  $^{53}\text{Cr}$ , and normal Mn and Ni were used, on Fe-20Cr-12Ni the tracers  $^{54}\text{Fe}$ ,  $^{53}\text{Cr}$ ,  $^{62}\text{Ni}$ , and normal Mn. The layers had a thickness of about 15 nm, estimated by weighing with a microbalance and by AES depth profiling.

For diffusion annealing, the samples were placed in quartz ampoules with a volume of about 2.5 ml. The ampoules were filled with purified and

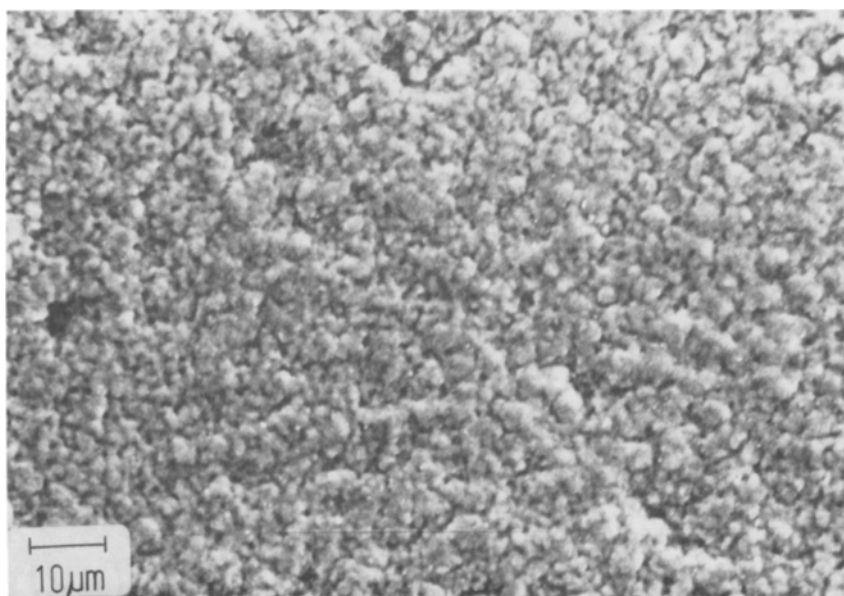


Fig. 4. SEM micrograph of a preoxidized surface of Fe-20Cr.

dried  $H_2$  having a dew point in the range of 233–228 K, i.e., an atmosphere with a ratio of  $P_{H_2O}/P_{H_2}$  close to the Cr–Cr<sub>2</sub>O<sub>3</sub> equilibrium at the annealing temperature of 1173 K. The exact value  $P_{H_2O}/P_{H_2} = 8.3 \times 10^{-5}$  presumably was achieved by equilibration with the Cr/Cr<sub>2</sub>O<sub>3</sub> couple. The ampoules were closed at a pressure of 0.30 bar and were afterward held at 1173 K; the annealing times varied from 10 min to 4 hr. In most of the diffusion runs, the annealing times were chosen so that the tracer did not reach the Cr<sub>2</sub>O<sub>3</sub>/alloy interface during the annealing process.

The depth profiles were determined by SNMS (sputtered neutral mass spectroscopy) using an Ar<sup>+</sup>-ion source. SNMS allows the analysis of conducting, semiconducting, and insulating surfaces and films with quantitative detection of all elements down to ppm concentrations. Since a low-pressure plasma is used as an ion source for sputtering of the samples and a post-ionizer for the sputtered neutrals, excellent depth resolution is combined with high detection sensitivity for all elements.<sup>24,25</sup> The method does not suffer from artifacts caused by preferential sputtering and matrix effects: by using primary ions of a few hundred eV the atomic mixing usually resulting from erosion by ion bombardment is avoided. The detection probability is similar for all elements and shows only small variations in different materials. Due to the advantages of this method, depth profiles measured by SNMS are an excellent method for the determination of diffusion coefficients, especially of those with small values.

The sputtering rate was determined by relating the thickness of the chromia layer to the sputtering time ( $t_s$ ) necessary for the sputtering from the sample surface to the chromia scale/alloy interface. Due to the roughness of the chromia layer, the sputter profile shows a broad transition zone from the chromia to the alloy. Therefore,  $t_s$  is defined as the sputtering time after which the O-peak reaches 50% of its height in pure chromia, at the same time  $t_s$  the Cr-peak height also reaches the value averaged of the peak heights in pure chromia and in the alloy. The sputtering rate for Cr<sub>2</sub>O<sub>3</sub> was found to be 0.8 nm/s (primary ion current for sputtering: 250  $\mu$ A, sample voltage: 600 eV).

## DATA ANALYSIS AND RESULTS

Figures 5 and 6 shows some of the penetration profiles measured. All profiles, using Fe, Cr, or Ni as tracers, have the same general shape: there are two parts of the profile with different slopes. Near the surface, the tracer concentration is relatively high and the mean concentration (logarithmic in arbitrary units) decreases proportional to the square of the penetration depth  $y$ . In this part, the profile is dominated by lattice diffusion. At higher penetration depths, the tracer concentration decreases to very low values. In this

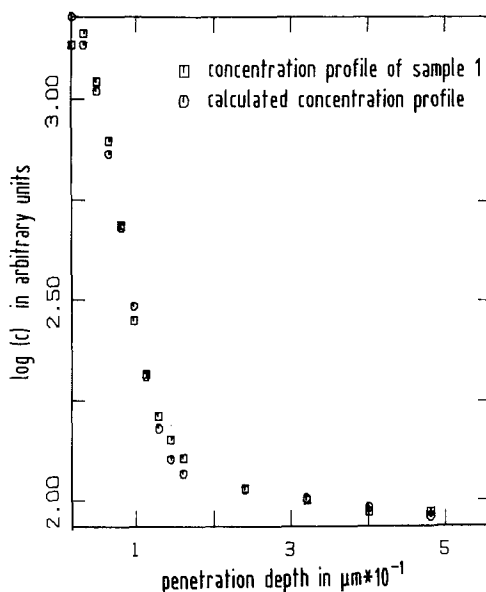


Fig. 5. Measured and calculated concentration profile of  $^{54}\text{Fe}$  in chromia grown on Fe-20Cr (Sample 1, see Table III).

diffusion tail, the slope is small and the logarithm of tracer concentration decreases almost linearly with penetration depth. This shape of the penetration profile is typical for B-type diffusion kinetics in which each boundary is assumed to be isolated and the flux at large distances from the boundary (parallel to the surface) approaches zero. This model can be applied when the bulk-diffusion distance is smaller than the grain size.<sup>26</sup>

A main difficulty in the measurement of grain-boundary diffusion in polycrystalline oxides is that a diffusion tail can also originate from penetration of tracer atoms into isolated dislocations. Both kinds of diffusion tails can be distinguished experimentally by the dependence of the slope of the tail on the annealing time  $t_a$ , in a plot of the logarithm of tracer concentration vs the penetration depth. LeClaire and Rabinovitch<sup>27</sup> have shown that the slope should be almost independent of the annealing time  $t_a$  for diffusion along isolated dislocations, whereas the slopes are proportional to  $t_a^{-1/4}$  for diffusion along grain boundaries.

For Cr and Ni as tracers, the latter proportionality is almost fulfilled; therefore it can be assumed that the diffusion tail in these experiments is due to grain-boundary diffusion. For Fe, the slope is neither proportional to  $t_a^{-1/4}$  nor independent of  $t_a$ . Perhaps grain-boundary diffusion of Fe is faster



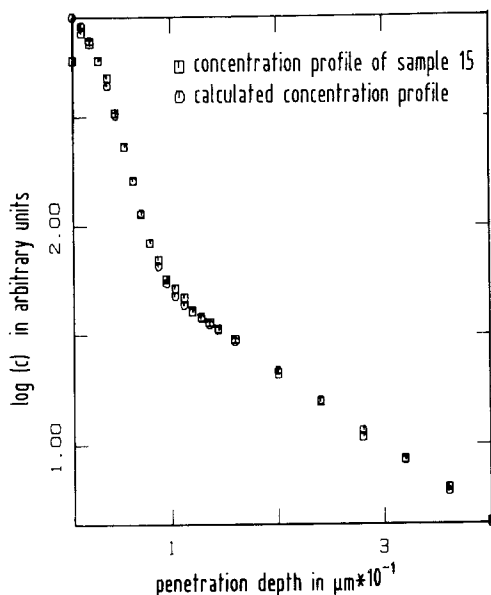


Fig. 6. Measured and calculated concentration profile of  $^{62}\text{Ni}$  in chromia grown on Fe-20Cr-12Ni (Sample 15, see Table III).

than expected, and therefore the diffusion tail was not completely recorded. Figure 7 shows the penetration profile for Mn diffusion in  $\text{Cr}_2\text{O}_3$  on Fe-20Cr-12Ni. In this profile, there is no diffusion tail. Obviously, the lattice diffusion of Mn is so fast that the contribution of grain-boundary diffusion can only be investigated with thicker  $\text{Cr}_2\text{O}_3$ -layers. (If the diffusion times would be chosen shorter than 10 min, the time necessary for heating up the sample would lead to a large error in the measurement of the diffusion time.)

In the analysis, the relation between the tracer concentration in the lattice ( $c$ ) and in the grain-boundary slab ( $c'$ ) at the edge of the boundary slab must be taken into account.<sup>28</sup> The amount of tracer evaporated onto the surface of the sample was very small (thickness about 15 nm). Therefore, the solubility of the tracer in the bulk will probably not be exceeded and it can be assumed that  $c = c'$  (segregation factor  $\gamma = c/c' = 1$ ).

For determination of the lattice-diffusion coefficient  $D$  and of the grain-boundary diffusion coefficient  $D'$  the model of Suzuoka<sup>29</sup> was applied. In this model, it is assumed that a thin uniform layer of the tracer is deposited on the surface and that this finite amount of material diffuses into the sample without any diffusion within the deposited layer parallel to the surface (finite-source condition). Suzuoka proposed an iterative process for the evaluation of  $D$ ,  $D' \cdot \delta$  ( $\delta$  = grain boundary width), and the grain size  $b$ .

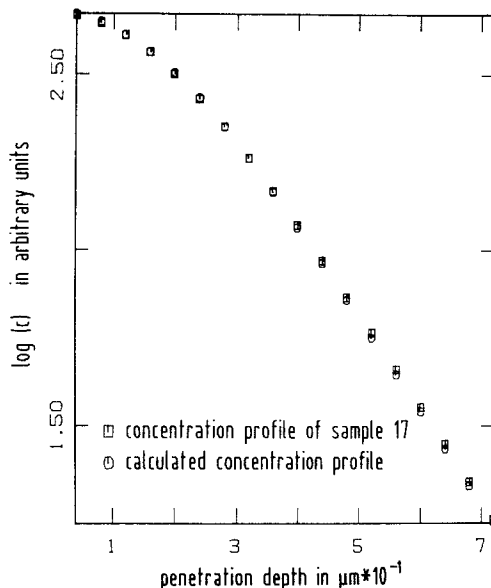


Fig. 7. Measured and calculated concentration profile of Mn in chromia grown on Fe-20Cr-12Ni (Sample 17, see Table III).

Information about the grain boundary width  $\delta$  is necessary for the calculation of  $D'$ . But there are only a few studies on the grain boundary width  $\delta$  in oxides. Atkinson and Taylor<sup>30</sup> estimated  $\delta = 0.7$  nm for NiO at 773 K. Here the results for  $D' \cdot \delta$  are reported.

The values for  $D$ ,  $D' \cdot \delta$ , and  $b$  are given in Table III. Figures 5–7 show examples of calculated concentration profiles in comparison to the experimentally measured profiles. The agreement of the measured and calculated profiles was very good for all diffusion runs.

For the tracers Fe, Cr, and Ni the values of  $D$  are 3–5 orders of magnitude smaller than the values of  $D'$ , if  $\delta = 0.5$  nm is assumed. This is in agreement with previous studies.<sup>17,20–22</sup> The calculated values of  $D$ ,  $D'$ , and  $b$  are different for varying annealing times. With increasing annealing time,  $D$  and  $D'$  seem to decrease and  $b$  seems to increase in most diffusion runs. Such a scatter of diffusivity values from different diffusion runs has also been found in other studies.<sup>30</sup> Atkinson and Taylor<sup>30</sup> in their calculation therefore used fixed values of  $D$  taken from experiments with monocrystals.

Reasons for this scatter might arise from the sputtering process, however, in applying the SNMS method, atomic mixing resulting from erosion by ion bombardment should be avoided. Another possible reason for the

**Table III.** Values of the Lattice-Diffusion Coefficient  $D$ , of the Product of Grain-Boundary-Diffusion Coefficient  $D'$  and Grain-Boundary Width  $\delta$ , and Grain-Size Parameter  $b$ <sup>29</sup>

Base alloy	Sample	Tracer	Annealing time	$D/\text{cm}^2 \text{s}^{-1}$	$D'\delta/\text{cm}^3 \text{s}^{-1}$	$b/\mu\text{m}$
Fe-20Cr	1	<sup>54</sup> Fe	15 min	$2 \times 10^{-14}$	$1 \times 10^{-16}$	0.11
	2		4 hr	$3 \times 10^{-15}$	—	0.21
	3	<sup>53</sup> Cr	15 min	$1 \times 10^{-14}$	$1 \times 10^{-16}$	0.09
	4		4 hr	$4 \times 10^{-16}$	$2 \times 10^{-17}$	0.06
	5	Ni	10 min	$3 \times 10^{-15}$	$2 \times 10^{-19}$	0.20
	6		17 min	$6 \times 10^{-15}$	$3 \times 10^{-18}$	0.29
	7		4 hr	$8 \times 10^{-16}$	$2 \times 10^{-19}$	0.58
	8	Mn	10 min	$2 \times 10^{-14}$	$2 \times 10^{-17}$	0.07
	9		17 min	$6 \times 10^{-14}$	$5 \times 10^{-17}$	0.55
	10		4 hr	$2 \times 10^{-15}$	$5 \times 10^{-18}$	0.20
Fe-20Cr-12Ni	11	<sup>54</sup> Fe	15 min	$4 \times 10^{-15}$	$1 \times 10^{-17}$	0.12
	12		4 hr	$7 \times 10^{-16}$	—	0.13
	13	<sup>53</sup> Cr	15 min	$7 \times 10^{-15}$	$2 \times 10^{-17}$	0.08
	14		4 hr	$8 \times 10^{-16}$	$5 \times 10^{-18}$	0.10
	15	<sup>62</sup> Ni	15 min	$5 \times 10^{-15}$	$5 \times 10^{-19}$	0.16
	16		4 hr	$4 \times 10^{-16}$	$1 \times 10^{-19}$	0.32
	17	Mn	15 min	$2 \times 10^{-13}$	—	0.39
	18		4 hr	$1 \times 10^{-14}$	—	1.19

deviation is the roughness of chromia layers grown on polycrystalline metallic samples. For the calculation of the diffusion coefficients, a flat surface is required. To get information about the influence of surface roughness and of artifacts during the sputtering process, Ni was deposited on a  $\text{Cr}_2\text{O}_3$ -layer grown on Fe-20Cr. This sample was analyzed by SNMS without a preceding diffusion anneal. The profile appears to show a bulk diffusion range of 25 nm. Therefore, the surface roughness was indeed a problem in this investigation. Another problem in this investigation could be evaporation of chromium or chromium oxides during diffusion annealing. But at the temperature used of 1173 K and the low oxygen pressure during the diffusion anneal the vapor pressure of possible gaseous species is very low.<sup>31</sup> As the volume of the ampoule is very small (2.5 ml), only negligible amounts of Cr,  $\text{CrO}$ ,  $\text{CrO}_2$ , or  $\text{CrO}_3$  can evaporate.

According to Suzuoka, the difference between calculated and real grain size  $b$  should be smaller than 30%. Atkinson and Pummery found in their investigations on NiO (Ref. 32) that the calculated grain size is about three times smaller than the real grain size and that the calculated values increase with annealing time. The same tendency was observed in this study. If the experiments are really B-type,<sup>26</sup> the values of  $(D'_a)^{1/2}$  must be smaller than  $2b$ . This is fulfilled in all diffusion runs. Therefore the solution of Suzuoka can be applied.

In spite of all the difficulties and uncertainties in this investigation, some general tendencies can be derived. Comparing the lattice-diffusion coefficients  $D$  of different tracers in  $\text{Cr}_2\text{O}_3$ , it can be seen that lattice diffusion of Mn is the fastest process. This is confirmed by the shape of the diffusion profile. The differences of  $D$  for Fe, Cr, and Ni are not distinct enough to lead to clear statements. Comparison of the grain-boundary diffusion coefficients shows that the value for Ni is the smallest. The  $D'$ -values for Fe and Cr are in the same range. Diffusion of the tracers in  $\text{Cr}_2\text{O}_3$  grown on different alloys does not show significant differences with the exception of Mn as tracer. The value of  $D_{\text{Mn}}$  in  $\text{Cr}_2\text{O}_3$  on Fe-20Cr-12Ni is about one order of magnitude higher than on Fe-20Cr. The observation that diffusion coefficients of Cr in chromia are almost independent of the alloy is in agreement with the results of Gil *et al.*<sup>33</sup> on the diffusion of Cr in  $\text{Cr}_2\text{O}_3$  scales preformed on Co-40Cr alloys. The absolute values of these self-diffusion coefficients do not significantly differ from those observed on pure chromium by Lillerud and Kofstad<sup>14</sup> with the same method.

In former studies the fast diffusion of manganese in chromia has already been predicted. Cox *et al.*<sup>34</sup> estimated diffusivities of different metals in  $\text{Cr}_2\text{O}_3$  assuming that the metals diffuse as ions along  $\text{Cr}^{3+}$ -lattice sites. They predicted that the diffusion coefficients should decrease in the order  $D_{\text{Mn}} > D_{\text{Fe}} > D_{\text{Ni}} > D_{\text{Cr}}$ . Wild<sup>35</sup> concluded from AES-measurements on growing  $\text{Cr}_2\text{O}_3$ -scales that Mn diffuses two orders of magnitude faster than Cr.

In several studies on sulfidation/oxidation of alloys different diffusion fluxes of metals in chromia layers have been observed, e.g., during sulfidation processes after preoxidation of chromia forming alloys.<sup>1-3,8</sup> According to Perkins,<sup>1-3</sup> manganese is one of the major elements contributing to the failure of alloys which form chromia scales in sulfidizing atmospheres due to outward diffusion of  $\text{Mn}^{2+}$  through the oxide layer, resulting in external growth of manganese sulfide.

During the oxidation of high-alloy steels in air with low-manganese concentrations, the formation of  $\text{MnCr}_2\text{O}_4$  on top of a  $\text{Cr}_2\text{O}_3$ -layer is generally observed.<sup>36</sup> As the concentration of manganese in the alloys is very low this fact can only be explained by very fast diffusion of manganese in chromia.

The very fast diffusion of Mn predicted by other authors is confirmed in this study applying a direct diffusion experiment. This study also shows that the differences of the flux of other cations like Fe or Cr through  $\text{Cr}_2\text{O}_3$ -layers cannot be explained by different diffusion coefficients.

## ACKNOWLEDGMENTS

This study was supported by the Deutsche Forschungsgemeinschaft (Gr 465-18/2). The analysis of the samples with SNMS at Hoesch Stahl AG, Dortmund (FRG) by Mr. H. Patotzki is gratefully appreciated.

## REFERENCES

1. R. A. Perkins, *Proceedings of the Conference on Corrosion/Erosion of Coal Conversion Materials*, A. V. Levy, ed. (NACE, January, 1979), p. 351.
2. R. A. Perkins, in *Proceedings of Conference on "Environmental Degradation of High Temperature Materials,"* Vol. 2, Spring Residential Conference (Chameleon Press, London, 1980) 5/1.
3. R. A. Perkins, in *Proceedings of Conference on "Environmental Degradation of High Temperature Materials,"* Vol. 2, Spring Residential Conference (Elsevier Applied Science Publishers Ltd., Chameleon Press, London, 1980) 5/17.
4. D. J. Baxter and K. Natesan, *Corros. Sci.* **26**, 153 (1987).
5. D. J. Baxter and K. Natesan, *Oxid Met.* **24**, 331 (1985).
6. I. Wolf, H. J. Grabke, and H. P. Schmidt, *Oxid Met.* **29**, 289 (1988).
7. I. Wolf and H. J. Grabke, *Solid State Commun.* **54**, 5 (1985).
8. R. E. Lobnig and H. J. Grabke, *Corros. Sci.* **30**, 1045 (1990).
9. R. E. Lobnig, H. P. Schmidt, and H. J. Grabke, *Mater. Sci. Eng.* **120**, 123 (1989).
10. D. Bramhoff and H. J. Grabke (unpublished results).
11. R. Lindner and A. Akerstrom, *Z. Phys. Chem. N.F. (Neue Folge)* **6**, 162 (1956).
12. D. V. Ignatov, I. N. Belokurova, and I. N. Beyanin, USA E. C. Report, NP-TR-448, 1958, p. 256.
13. W. C. Hagel and A. U. Seybolt, *J. Electrochem. Soc.* **108**(12), 1146 (1961).
14. K. P. Lillerud and P. Kofstad, *Oxid. Met.* **17**, 127, 177, 195 (1982).
15. L. C. Walters and R. E. Grace, *J. Appl. Phys.* **8**, 2332 (1965).
16. K. Hoshino and N. L. Peterson, *J. Am. Ceram. Soc.* **66**, C-202 (1983).
17. A. Atkinson and R. I. Taylor, in *Transport in Nonstoichiometric Compounds*, G. Simdkovich and G. Stubican, ed. (Plenum Publishing Corporation, New York, 1985), p. 285.
18. D. Schwanke, Komponentendiffusion und Fehlordnung in  $\text{Cr}_2\text{O}_3$ , Dissertation, Erlangen, 1986.
19. P. Kofstad, *High Temperature Corrosion* (Elsevier Applied Science Publishers Ltd., Barking, Essex, U.K., 1988).
20. H. G. Sockel, B. Saal, and M. Heilmaier, *Surf. Interface Anal.* **12**, 531 (1988).
21. A. C. S. Sabioni, B. Lesage, A. M. Huntz, J. Besson, C. Dolin, and C. Monty, *Grain Boundary Diffusion in  $\text{Cr}_2\text{O}_3$*  (to be published).
22. J. H. Park, W. E. King, and S. J. Rothman, *J. Am. Soc.* **70**(12), 880 (1987).
23. R. D. Kinloch, Cation Tracer Diffusion in Chromium Sesquioxide, Ph.D. thesis, University of Delaware, University Microfilms, Ann Arbor, Michigan, June 1970.
24. R. Jede, K. Seifert, and G. Dünnebier, *Anal. Chem.* **329**, 116 (1987).
25. R. Jede and H. Peters, *Techn. Messen tm* **54**, 343 (1987).
26. L. G. Harrison, *Trans. Faraday Soc.* **57**, 1191 (1961).
27. A. D. LeClaire and A. Rabinovitch, *J. Phys. C, Solid State Phys.* **14**, 3863 (1981).
28. N. L. Peterson, *Int. Met. Rev.* **28**, 65 (1983).
29. T. Suzuoka, *Trans. Jpn. Inst. Met.* **2**, 25 (1961).
30. A. Atkinson and R. J. Taylor, *Phil. Mag. A* **43**, 979 (1981).
31. N. Birks and G. H. Meier, *Introduction to High Temperature Oxidation of Metals* (Edward Arnold Publishers Ltd., London, 1983).
32. A. Atkinson and F. C. W. Pummery, in *Transport in Nonstoichiometric Compounds*, S. Simkovitch and V. S. Stubican, eds. (New York, 1985).
33. A. Gil, S. Mrowec, J. Jedlinski, and G. Borchardt, *Solid State Ionics* (submitted).
34. M. G. E. Cox, B. McEnaney, and V. D. Scott, *Phil. Mag.* **26**, 839 (1972).
35. R. K. Wild, *Corros. Sci.* **17**, 87 (1977).
36. K. Ledjeff, A. Rahmel, and M. Schorr, *Werkst. Korros.* **30**, 767 (1979).